JOC The Journal of Organic Chemistry

Featured Article

pubs.acs.org/joc

Intramolecular General Base Catalysis in the Hydrolysis of a Phosphate Diester. Calculational Guidance to a Choice of Mechanism

Anthony J. Kirby,*[,†] Michelle Medeiros,[‡] José R. Mora,[‡] Pedro S. M. Oliveira,[‡] Almahdi Amer,[§] Nicholas H. Williams,*[,§] and Faruk Nome*[,‡]

[†]University Chemical Laboratory, University of Cambridge, Cambridge CB2 1EW, U.K.

[‡]Departamento de Química, Universidade Federal de Santa Catarina, 88040-900 Florianópolis, SC, Brazil

[§]Centre for Chemical Biology, Department of Chemistry, University of Sheffield, Sheffield S3 7HF, U.K.

Supporting Information

ABSTRACT: Notwithstanding its half-life of 70 years at 25 °C, the spontaneous hydrolysis of the anion of di-2-pyridyl phosphate (**DPP**) is thousands of times faster (ca. 3000 at 100 °C, over 10000-fold at 25 °C) than expected for a diester with leaving groups of pK_a 9.09. The kinetic parameters do not permit a conclusive choice between five possible mechanisms considered, but the combination of kinetics and calculational evidence supports a single-step, concerted, $S_N2(P)$ mechanism involving the attack of solvent water on phosphorus assisted by intramolecular catalysis by a (weakly basic) pyridine nitrogen acting as a general base. Catalysis is relatively efficient for this mechanism, with an estimated effective molarity (EM) of the general base of >15 M, consistent with the absence of catalysis by typical buffers. Further new results confirm that varying the nonleaving group has minimal effect on the rate of spontaneous diester hydrolysis, in striking contrast to the major effect on the corresponding reaction of triesters: though protonation of one nitrogen of DPP^- increases the rate of hydrolysis by 6 orders of magnitude, in line with expectation.

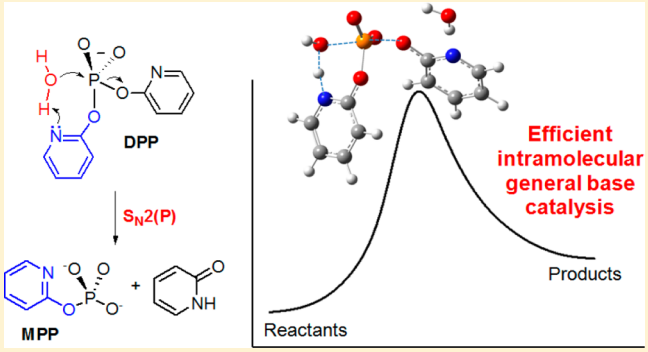

INTRODUCTION

We recently reported[1] "first results" of an investigation prompted by the intriguing report of Liu and Wulff[2] that their attempt to prepare di-2-pyridyl phosphate (DPP) as a new template "failed owing to its instability". 2-Hydroxypyridine, which exists in water almost exclusively as 2-pyridone (Scheme 1), has a nominal pK_a of 9.09,[3] and its anion is not obviously a good leaving group. So this apparent instability suggested that the neighboring pyridine nitrogens could be involved in intramolecular catalysis. The geometry is not favorable for intramolecular nucleophilic catalysis, which would involve the formation of a four-membered ring, but the system appears to be well set up for intramolecular general base catalysis (IGBC, Scheme 2), and we initiated an investigation of the catalytic properties of the 2-pyridyl group in phosphate esters.

Scheme 1. Equilibria Involving 2-Hydroxypyridine[3]

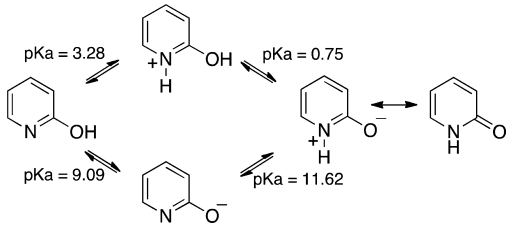

Scheme 2. Suggested Special Mechanism for "Efficient" Intramolecular GBC of the Hydrolysis of TPP[1]

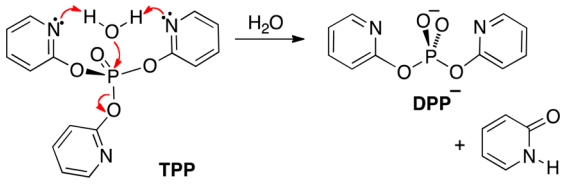

Our first results were for the triester TPP, which we found to be hydrolyzed near pH 7 some 10^7 times faster than expected on the basis of a linear free energy relationship derived for dialkyl aryl phosphate triesters. However, we soon established that this enhanced reactivity is fully accounted for by the activating electronic effects of the aromatic nonleaving groups[4] so that there is no need to invoke intramolecular catalysis.

We now report our results with the diester DPP, the original target of the investigation. We confirm that the hydrolysis of

Received: November 21, 2012
Published: February 1, 2013

   dx.doi.org/10.1021/jo302498g | J. Org. Chem. 2013, 78, 1343−1353

the DPP anion is very slow, as shown previously by Brown and Zamkanei,[5] who found that DPP^- was "not hydrolysed" under their mild conditions (pH 6−8, 37 °C, in the presence or absence of Co(2+) or selected complexes). But we find that DPP does exhibit significantly enhanced reactivity, consistent with intramolecular catalysis of hydrolysis. We discuss the mechanism of its hydrolysis, via the more reactive monoester MPP, to inorganic phosphate (Scheme 3) and present new information on the more general question of the effect of the nonleaving group on diester reactivity.

Scheme 3. Hydrolysis Reaction of Di-2-pyridyl Phosphate (DPP)

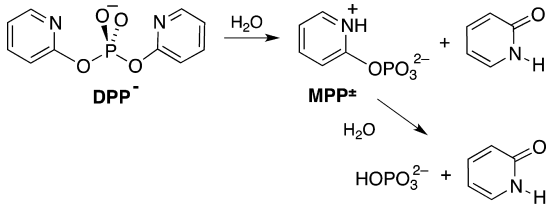

RESULTS AND DISCUSSION

Nonleaving Group Effects on Diester Hydrolysis. Identifying the remarkably large effects of varying the nonleaving (so-called "spectator") groups on the rates of hydrolysis of phosphate triesters[4] prompted us to look again at their apparently minimal effects on the reactions of diesters. The original two-point comparison[6] was based on the observation that bis-2,4-dinitrophenyl phosphate was hydrolyzed at 39 °C, only 2.88 times faster than the methyl 2,4-dinitrophenyl ester, little more than the statistical factor of 2. We have extended the data set to four diesters $RO(PO_2^-)$−O-2,4-DNP, with R = Me, Ph, 4-nitrophenyl, and 2,4-dinitrophenyl, with 2,4-dinitrophenol being the common leaving group. The data and the Brønsted (nonleaving group) plot are presented in the Supporting Information (Table S.1.5 and Figure S.1). The minimal dependence of the rate of spontaneous hydrolysis on the nonleaving group RO is confirmed by the new measurements of k_0 at 100 °C, which are correlated by a β_{NLG} of −0.031 ± 0.001 for the four compounds. The contrast with triesters, with β_{NLG} of −0.35 ± 0.02 per nonleaving group at 25 °C,[4] is striking.

Hydrolysis of DPP. The pH−rate profile for the hydrolysis of DPP (Figure 1) shows acid and base-catalyzed limbs separated by a hint of a pH-independent region: the observed rate at the pH 9.4 minimum was 4−5 times faster than calculated for the sum of the acid- and base-catalyzed reactions of the anion (curve labeled k_{calc} in Figure 1). Furthermore, this rate is over 10000 times faster than predicted for the spontaneous hydrolysis of a simple diaryl phosphate diester with leaving groups of pK_a = 9.09.[7] (For details, see the Supporting Information). Other things being equal, this degree of acceleration would have been expected to generate a significant pH-independent region in the rate profile, but, as a result of the high reactivity of the N-protonated form $DPP^{\pm}$ (Scheme 4), the rate minimum is shifted to higher pH (9−10) compared with rate profiles for other diaryl phosphates, which typically show minima in the region of pH 4−5.[7]

Phosphate diesters are well-known to be the least reactive esters of phosphoric acid in the absence of acid or base: in a comparable system, the spontaneous hydrolysis of diphenyl

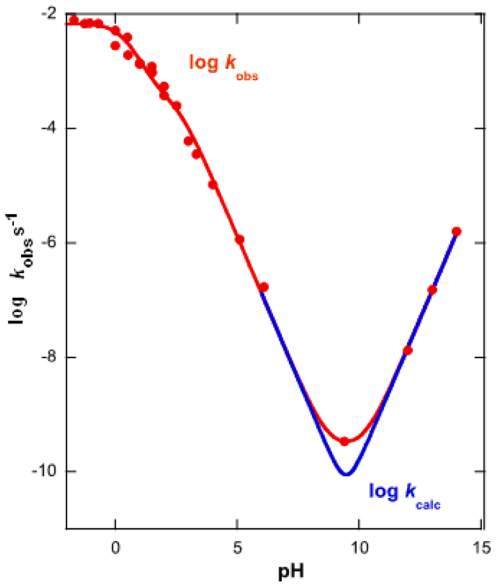

Figure 1. pH−(log) rate profile for the hydrolysis of DPP at 25 °C and ionic strength 1.0 M (KCl). The points for k_{obs} are experimental; the curves are calculated using the rate constants and pK_a's shown in Table 1 but setting k_0 to zero for k_{calc}. For full data see the Supporting Information.

Scheme 4. Three Ionic Forms of DPP Significant in the pH Region

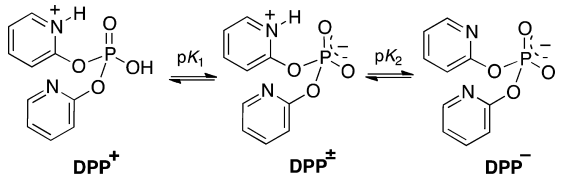

phosphate was found to be too slow to measure at 100 °C.[7] We made extensive efforts to measure the rate of the reaction for DPP^- directly at 25 °C, using the method of initial rates, finding levels of random error over numerous experiments to be frequently unacceptable. The rate constant quoted in Table 1 (corresponding to a half-life of 70 years) is the result of a

Table 1. Kinetic Data (Rate Constants and pK_a's) Derived from the pH−rate Profile of Figure 1 for the Hydrolysis of Di-2-pyridyl Phosphate DPP at 25 °C and Ionic Strength 1.0 M (KCl)[a]

ionic form	rate constants	pK_a	pK_{LG}[b]
DPP^+	k_H = 6.81 ± 0.89 x10^{-3} s^{-1}	0.33 ± 0.2	0.75
$DPP^{\pm}$	$k_{\pm}$ = 3.56 ± 0.44 x10^{-4} s^{-1}	2.73[c]	0.75
DPP^-	k_0 = 3.12 ± 0.85 x10^{-10} s^{-1}; k_{OH} = 1.47 ± 0.26 × 10^{-6} $M^{-1}s^{-1}$		9.09

[a]A complete data set is in Table S.1.1 of the Supporting Information. [b]Literature value.[3] [c]Measured value.

cognate series of best measurements, made in parallel at different buffer (mainly CHES) concentrations at the pH minimum of 9.4−9.7, using the maximum practical substrate concentrations (for details see the Experimental Section). The measurements cited gave acceptably reproducible rate constants at 25 °C and support the following conclusions: (1) The rate at the pH minimum is (marginally) too high to be explained by

dx.doi.org/10.1021/jo302498g | J. Org. Chem. 2013, 78, 1343−1353

the sum of the hydroxide and acid-catalyzed reactions (Figure 1). (2) There is no catalysis by standard buffers of pK_a < 10. The presence or absence of measurable buffer catalysis of hydrolysis is a simple, but generally reliable test of intramolecular catalytic efficiency.[4] (3) The initial product, the monoester MPP (Scheme 3), is hydrolyzed faster than DPP between pH 1.2 and 12 (Figure 2), so initial rate calculations

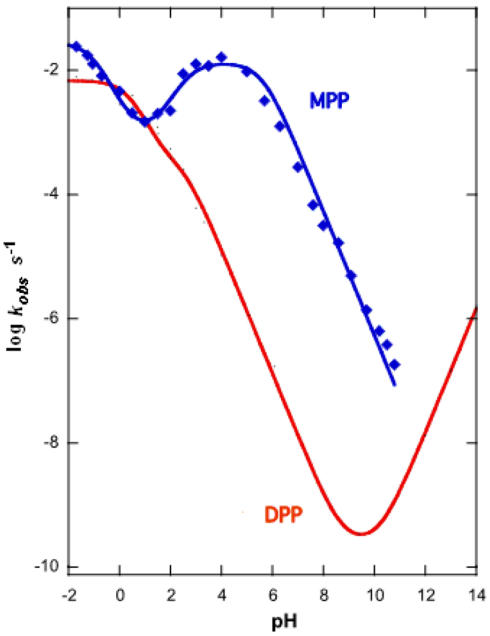

Figure 2. pH profiles compared for the hydrolysis of DPP (curve from Figure 1) and the product MPP. The points are experimental; the curves are calculated from the data in Table 1.

are based in most cases on the release of 2 equivalents of 2-pyridone. Where the rates of the sequential reactions are closely similar, rate constants are derived from the appropriate equation for consecutive first-order reactions, as described in the Supporting Information. The corrections turn out to be small.

The hydrolysis of MPP is itself of interest as a model for the general mechanism of hydrolysis of phosphate monoester monoanions but presents no obvious problems of measurement or interpretation and will discussed in more detail elsewhere.

The spontaneous hydrolysis is (by far) the slowest reaction of DPP, so should be better defined, and more easily measured, at higher temperatures. We have measured the rate of hydrolysis, specifically at the pH minimum, under our standard conditions, of pH 9.4–9.7 and buffer at 25 °C (see the Experimental Section), at a range of temperatures up to and including 100 °C. The data for k_{obs} (Table 2) give an excellent linear Eyring plot, consistent with a constant mechanism over the range 25–100 °C, and the thermodynamic parameters are shown in Table 2. For the reaction at 100 °C the release of 2-pyridone and the disappearance of DPP were followed to completion, using HPLC. The rate measured at 100 °C is also faster than predicted, on the basis of a linear free energy relationship measured specifically for diaryl phosphate esters at 100 °C,[7] by a factor of ca. 3000.

We interpret the log k_{obs}/pH rate-profile of Figure 1 in terms of reactions of the three ionic forms shown in Scheme 4 (above), according to eq 1.

Table 2. Kinetic Data for the Hydrolysis of Di-2-pyridyl Phosphate anion DPP$^-$, at the pH Minimum (9.4–9.7 at 25°C): In CHES Buffer, Ionic Strength 1.0 M (KCl) at a Range of Temperatures

pH	T (°C)	k_{obs} (s^{-1})	pH	T (°C)	k_{obs} (s^{-1})
9.4	25	3.12×10^{-10}	9.7	75	1.35×10^{-7}
9.4	45	5.44×10^{-9}	9.7	90	8.50×10^{-7}
9.7	60	3.70×10^{-8}	9.7	100	2.06×10^{-6a}

[a]Measured by HPLC. $\Delta H^{\ddagger}$ = 25.1 ±0.5 kcal/mol, $\Delta S^{\ddagger}$ = −17.8 ±1.6 cal/K/mol, $\Delta G^{\ddagger}$ = 30.4 kcal/mol, at 25 °C.

Table 3. Solvent Isotope Effect Measurements: Parallel Runs in Triplicate in CHES Buffer, pH 9.4, Ionic Strength 1.0 M (KCl)

	mean k_{obs} (s^{-1})	k_{H2O}/k_{D2O}
DPP$^-$ in H_2O, 25 °C	$3.37 \pm 0.28 \times 10^{-10}$	k_H/k_D(25 °C) = 1.28 ± 0.22
DPP$^-$ in D_2O	$2.64 \pm 0.53 \times 10^{-10}$	
DPP$^-$ in H_2O, 45 °C[b]	1.51×10^{-8}	k_H/k_D (45 °C) = 1.20
DPP$^-$ in D_2O	1.26×10^{-8}	

[b]Single measurements at 45 °C. For full data see the Supporting Information.

$$k_{obs} = k_H[DPP^+] + k_{\pm}[DPP^{\pm}] + k_0[DPP^-] + k_{OH}[HO^-]\cdot[DPP^-] \quad (1)$$

Below pH 5 the profile (Figure 1) is not a straight line of slope −1 but shows inflections near pH 3 and pH zero indicative of two ionisations. The reaction at acid pH (<2) represents the hydrolysis of DPP$^+$; while between pH 2.5 − 5 we see the reaction of the zwitterionic species DPP$^{\pm}$ (the independently measured pK_2 of the pyridyl group is 2.73). This is the ionization responsible for the marked shift of the rate minimum to higher pH evident for the hydrolysis of DPP. The reactions above pH 9 are the spontaneous and alkaline hydrolysis of DPP$^-$.

Two rate constants in the pH region are unusually high for a phosphodiester with leaving groups of pK_a 9.09. That for the hydrolysis of DPP$^{\pm}$ is simply explained: protonation of a pyridyl N converts the leaving group to 2-pyridone, a species over eight powers of ten less basic than its anion. In terms of a β_{LG} (leaving group) above unity the observed rate difference (only 10^6-fold faster than DPP$^-$) is consistent with a significant rate enhancement for the reaction of the anion. As described above, k_0 for the spontaneous hydrolysis of the anion DPP$^-$ is indeed significantly faster than expected at 25 °C: the observed value of k_0 at the pH minimum is estimated to be some 10000 times faster than estimated for the diester of a phenol of pK_a = 9.09. (See the Supporting Information.)

Activation Parameters. Table 4 compares enthalpies and entropies of activation for the spontaneous hydrolysis of DPP$^-$ with those for the same reaction of representative dialkyl and diaryl phosphodiesters taken from the literature. BMIPP$^{\pm}$ (bis[2-(1-methyl-1*H*-imidazolyl)phenyl] phosphate) is included because it is known to be hydrolyzed with a combination of intramolecular nucleophilic and general species catalysis involving two (imidazole) nitrogens.[8]

The sequence illustrates very clearly the powerful effect of efficient intramolecular nucleophilic catalysis by imidazole N, expressed in both enthalpic and entropic terms for BMIPP, and worth 8.6 kcal mol^{-1} in $\Delta G^{\ddagger}$. The relatively modest

dx.doi.org/10.1021/jo302498g | J. Org. Chem. 2013, 78, 1343–1353

Table 4. Activation Parameters for the Spontaneous Hydrolysis of Selected Phosphate Diester Anions

		spontaneous hydrolysis (k_0)		
ester	reaction	$\Delta H^{\ddagger}$ (kcal mol^{-1})	$\Delta S^{\ddagger}$ (cal mol^{-1} K^{-1})	ref
dimethyl phosphate	(C–O cleavage)	(25.0)	(−16.8)	9
dineopentyl phosphate	(P–O cleavage)	29.5	−28.9	10
DPP	(P–O cleavage)	25.1 ± 0.5	−17.8 ± 1.6	Table 2
BDMIPP$^{\pm}$	(P–O cleavage)	19.0 ± 1.2	−9.05 ± 0.5	11
bis-2,4-DNPP	(P–O cleavage)	19.0	−25.5	7

acceleration of the hydrolysis of DPP$^-$ is fully accounted for by an increase in the entropy of activation.

Intramolecular Catalysis. The significant rate accelerations of the spontaneous hydrolysis of DPP$^-$ at 25 and 100 °C is prima facie evidence for participation in the reaction by the pyridine nitrogen(s). Several possible mechanisms suggest themselves. (i) A reaction involving the attack of hydroxide on the conjugate acid DPP$^{\pm}$ (Scheme 5, Nu = HO$^-$), which is

Scheme 5. Strong Nucleophiles Such As Hydroxide (Mechanism (i)) Could React Faster, Even at High pH, with Very Small Amounts of DPP$^{\pm}$ present, than with the Predominant DPP Anion

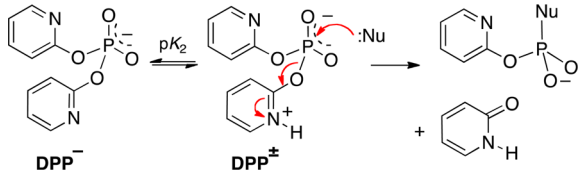

kinetically equivalent to the direct attack of the water on DPP$^-$. (ii) Intramolecular nucleophilic catalysis by the pyridine nitrogen of the nonleaving group. (iii) Direct attack of water on the DPP$^-$ anion, presumably (iv) with assistance from a pyridine nitrogen, acting as a general base.

In the context of mechanism i, it is important to notice that the relevant pre-equilibrium (DPP$^-$ + H_2O ⇌ DPP$^{\pm}$ + OH$^-$), is controlled by a large difference in acidity between water and DPP$^{\pm}$, consistent with a value of pK_2 of about 13 and, therefore, lies very much on the side of DPP$^-$ + H_2O as a global minimum. In order to check the viability of the reaction, we discuss first the observable reactions of DPP with external buffers, acting as nucleophiles (Scheme 5).

Reactions with Nucleophiles. The first indication that the spontaneous hydrolysis of TPP could not be subject to efficient intramolecular catalysis was our observation of buffer catalysis in the pH-independent region.[4] Buffer acids and bases are typically stronger acids, bases and nucleophiles than neutral water, but are not expected to compete with efficient intramolecular catalysis.[12] We looked very carefully for indications of catalysis of the hydrolysis of DPP$^-$ by typical buffer species (TRIS, CHES, etc.): we find none at 25, 45 or even 75 °C (see the Experimental Section). Typically rates are slightly reduced at higher buffer concentrations, suggesting that these are medium effects. Medium effects could also account for the weak rate increase observed near pH 10 at 70 °C with increasing [carbonate], but measurable catalysis under these conditions by this, the most basic buffer used, is not unexpected.

Mechanisms ii and iv: Intramolecular Catalysis. Why should intramolecular catalysis be observed for the spontaneous hydrolysis of DPP when we see little or none for the reaction of TPP? An important difference is that the pyridine nitrogens of DPP$^-$ are significantly more basic, with pK_a = 2.73 compared with −0.22 for TPP.[1] The rate enhancements (of the order of 10000 and 3000 at 25 and 100 °C) are substantial, and might suggest nucleophilic rather than general base catalysis by the neighboring pyridine N. Effective molarities (EM)[12] are not available for general base catalysis (GBC) of phosphate diester hydrolysis by pyridines (because the observed intermolecular reactions are primarily nucleophilic[6]), but we can make an informed estimate, of ca. 14 M, for the EM required to account for the observed rate of hydrolysis of DPP$^-$ by a pyridine of pK_a 2.73 by intramolecular nucleophilic catalysis (for details of the calculation, see the Supporting Information).

In the case of DPP$^-$, intramolecular nucleophilic catalysis would involve a 4-membered ring intermediate (Scheme 6),

Scheme 6. Mechanism (ii): Intramolecular Nucleophilic Catalysis of the Hydrolysis of DPP by Pyridine Nitrogen[a]

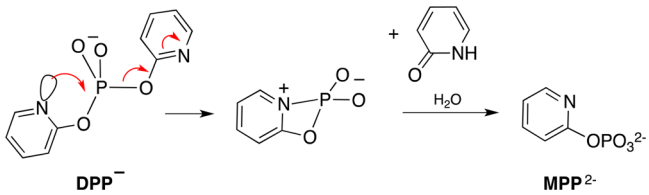

[a]The reactive intermediate formed would be converted rapidly to product by the attack of water on the central phosphorus atom.

and a low EM would be expected: so the estimate of 14 M is inconclusive. However, a similar EM would be expected for the reaction of DPP$^{\pm}$, with identical geometry for intramolecular nucleophilic attack. An estimated EM for this system, with a much better leaving group but more weakly basic nucleophile, is a barely significant 0.05 M (see the Supporting Information), which makes this mechanism a good deal less likely also for the DPP$^-$ reaction. Kinetic evidence consistent, though not uniquely consistent, with intramolecular nucleophilic catalysis is the low solvent deuterium isotope effect k_{H2O}/k_{D2O} = 1.28 ± 0.22 at 25 °C (Table 3). However, this figure is not conclusively smaller than the solvent deuterium isotope effect of 1.55 observed at 39 °C for the presumed $S_N2(P)$ hydrolysis of bis-2,4-dinitrophenyl phosphate.[7] (For further discussion of the solvent kinetic isotope effect, see below.) The entropy of activation, of $\Delta S^{\ddagger}$ = −17.8 cal mol^{-1} K^{-1}, is also inconsistent with a unimolecular transition state, though higher than expected for a spontaneous $S_N2(P)$ reaction involving solvated water as the nucleophile.

$S_N2(P)$ Mechanisms iii. The "default" mechanism for the spontaneous hydrolysis of a diaryl phosphate involves the concerted displacement of the leaving group by a water molecule, assisted by its hydrogen-bonded solvation partners acting as general bases to disseminate the developing positive charge into bulk solvent. There is general agreement that the hydrolysis reactions of phosphate diesters with good leaving groups do not involve pentacovalent phosphorane dianion intermediates.[13]

dx.doi.org/10.1021/jo302498g | J. Org. Chem. 2013, 78, 1343−1353

The evidence from kinetics tells us that the spontaneous hydrolysis of DPP^- is subject to moderately efficient catalysis, presumably involving neighboring pyridine nitrogen: and suggests strongly that the reaction involves water as the immediate nucleophile involved in nucleophilic attack on the DPP anion. Since the observed intermolecular reactions of pyridines with reactive diesters are primarily nucleophilic, the rate constants define only upper limits for general base catalysis: so that the EM of the order of 14 M estimated above for nucleophilic catalysis would represent a lower limit (and at the same time a relatively high value[12]) for IGBC. However, the kinetic evidence does not offer unambiguous support for one particular mechanism. So we have performed calculations for all the candidate mechanisms for the spontaneous hydrolysis of DPP^-: which do allow an informed choice. As a basis for comparison we performed a parallel calculation for the reaction of the simple diaryl ester bis-4-chlorophenyl phosphate ($4ClPP^-$), derived from a phenol with pK_a (9.38) close to that of 2-hydroxypyridine.

Computational Methods and Models. Density functional theory (DFT) calculations for the hydrolysis reactions of DPP^- and $4ClPP^-$ were performed at the B3LYP/6-31++G(d,p) level of theory using the GAUSSIAN 09 package implemented in Linux operating systems.[14] The default parameters for convergence, viz. the Berny analytical gradient optimization routine, were used; convergence on the density matrix was 10^{-9} atomic units, the threshold value for maximum displacement was 0.0018 Å, and the maximum force 0.00045 hartree/bohr. The energy minimum and the transition state were identified in each case, and their structures characterized by frequency calculations at 1 atm and both 298.15 and 373.15 K.[15] Since solvent effects are important, and indeed crucial when the solvent is a reactant, we optimized the substrate structures using the SCRF keyword and the polarizable continuum model (PCM) and the solvation model density (SMD).[16] The effects of adding a series of up to 5 explicit water molecules were examined, as we have reported recently in related systems.[17,18] Transition states (TS) were obtained by the quadratic synchronous transit (QST) protocol, and identified by the single imaginary frequency. Intrinsic reaction coordinates (IRC) were computed to confirm the reaction paths.

Thermodynamic Parameters. We calculated potential energy surfaces (PES) for the hydrolysis mechanisms of interest. Stationary points are located to characterize reactants (R), transition states (TS), intermediates, and products and thus to obtain activation parameters (Table 5). Five possible mechanisms were considered. The calculation for mechanism i, the kinetically equivalent reaction of hydroxide with $DPP^{\pm}$ (Scheme 5) gave one of the highest free energies of activation, confirming the tentative conclusion reached above from the kinetic results, that this mechanism could be excluded. As previously discussed, the relevant pre-equilibrium ($DPP^- + H_2O \rightleftharpoons DPP^{\pm} + OH^-$), is consistent with pK_2 ~13 and with $DPP^- + H_2O$ as a global minimum. In this sense, the energy barrier was determined with respect to this global minimum, resulting in a free energy of activation of 37.4 kcal/mol, which is consistent with a very slow reaction.

Mechanisms ii, iiia, iiib, and iv (Schemes 7–9) were considered in more detail. Mechanism ii is the two-step process involving intramolecular nucleophilic attack by a pyridine nitrogen via a 4-membered cyclic transition state, as described in Scheme 6. The reactive intermediate formed would be converted rapidly to product by the attack of water on the central phosphorus atom, so this step not involved in the

Table 5. Activation Free Energies and Rate Constants for the Hydrolysis of DPP^- at 25 °C Calculated at the B3LYP/6-31++G(d,p) Level of Theory

mechanism	$10^{10}k_{calc}$ (s^{-1})	$\Delta G^{\ddagger}$ (kcal/mol)
mechanism i ($1H_2O$)	4.16×10^{-7}	39.8
mechanism i ($3H_2O$)	2.39×10^{-5}	37.4
mechanism ii ($0H_2O$)	1.98×10^{-3}	34.8
mechanism ii ($1H_2O$)	2.54×10^{-4}	36.0
mechanism ii ($2H_2O$)	7.20×10^{-5}	36.8
mechanism iiia ($1H_2O$)	4.84×10^{-7}	39.7
mechanism iiia ($2H_2O$)	5.24×10^{-4}	35.6
mechanism iiia ($3H_2O$)	2.82×10^{-3}	34.1
mechanism iiia ($4H_2O$)	2.42×10^{-3}	33.3
mechanism iiia ($5H_2O$)	4.48×10^{-3}	34.3
mechanism iiib ($1H_2O$)	3.62×10^{-7}	39.9
mechanism iv ($1H_2O$)	1.72×10^{-2}	33.5
mechanism iv ($2H_2O$)	0.84 [5630][a]	31.2 [32.7][a]
mechanism iv ($3H_2O$)	0.52	31.5
observed	3.12 [16.000][a]	30.4 [31.7][a]

[a]Values in square brackets correspond to k_{calc} and $\Delta G^{\ddagger}$ calculated at 100 °C.

Scheme 7. Mechanism iiia: $S_N2(P)$ Mechanism for Hydrolysis Using a Single Water Molecule

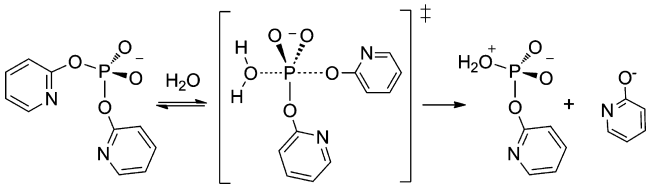

Scheme 8. Mechanism iiib: Two-Step Mechanism via a Pentaoxyphosphorane Intermediate Using a Single Water Molecule

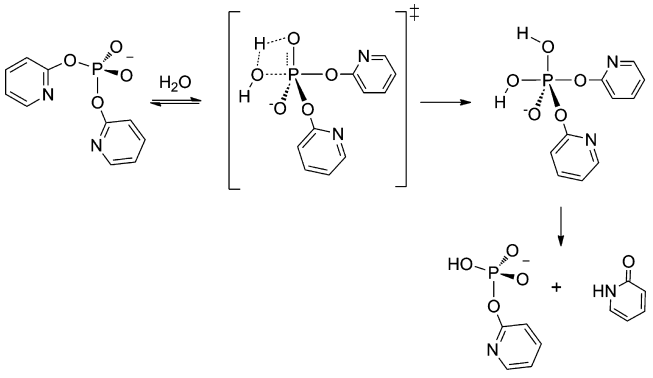

Scheme 9. Mechanism iv: $S_N2(P)$ Mechanism for Hydrolysis Using a Single Water Molecule with General Base Catalysis by a Nitrogen Atom of the Non-Leaving Group

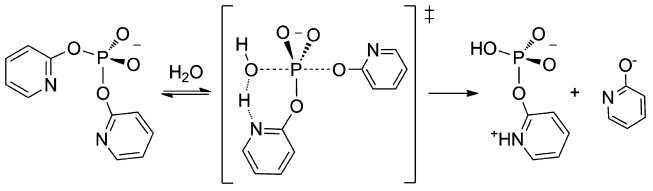

dx.doi.org/10.1021/jo302498g | J. Org. Chem. 2013, 78, 1343–1353

calculation). In the absence of an explicit water molecule, mechanism ii naturally shows the lowest activation energy (Table 5); but the calculated free energy of activation *increases* as water molecules are added to the calculation, and it immediately becomes the least favored of the remaining pathways. Since the reaction is carried out in water this mechanism can also be discarded with some confidence.

Mechanism iii involves attack by water oxygen on phosphorus following either (a) a classical concerted $S_N2(P)$ mechanism or (b) a two-step displacement of the leaving group, proceeding with formation of a pentacovalent addition intermediate, similar to that described for the hydrolysis reactions of phosphate triesters.[17,18] Finally, mechanism iv involves attack by a water oxygen atom on phosphorus assisted by general base catalysis by the nitrogen atom of the nonleaving group. Table 5 compares initial calculated and experimentally observed parameters for all the mechanisms considered.

For the $S_N2(P)$-based mechanisms iii, the addition of discrete waters to the calculation leads to a decrease in the free energy barrier, which for the concerted mechanism iiia levels out at 3–5 H_2O to give a value of $\Delta G^{\ddagger}$ 3–4 kcal·mol^{-1} above that observed experimentally. (A parallel calculation, described below, for the comparable diaryl ester bis-4-chlorophenyl phosphate (4ClPP$^-$), gave a calculated rate close to that expected for the 4-chlorophenoxide leaving group.)

The calculation for the two-step mechanism (iiib), involving a single H_2O and the formation of a pentaoxyphosphorane addition intermediate, found a transition state with a free energy of activation similar to that found for the concerted $S_N2(P)$ mechanism. However, all attempts to optimize the structure of the pentacoordinate intermediate led to cleavage of the P–O_{LG} bond and reversion to the bimolecular TS. The P–O_{LG} bond was longer in the hypothetical intermediate (1.824 Å) than in the transition state (1.690 Å), indicating that the phosphorane is not an energy minimum. Adding two and three water molecules to the calculation did not affect this result. Thus, the two-step mechanism (iiib) is not supported by the calculations. Similar results for phosphate diester hydrolysis have been widely discussed in the literature.[19a,20] Notice that it is possible to find pentacoordinate intermediates for phosphate diester hydrolysis under strongly acidic conditions,[19a] where these compounds are present in a neutral form, and so can behave like triesters.[17,18] Similarly, in the acid-catalyzed and spontaneous hydrolysis of dineopentyl phosphate, a compound with a rather poor leaving group, a stepwise addition–elimination mechanism was consistent with the theoretical calculations.[19b]

For mechanism iv, involving intramolecular general base catalysis by the nitrogen center of the nonleaving group, the calculated free energy of activation is in good agreement with the experimental value when two or three discrete water molecules are present. This mechanism accounts satisfactorily for the rate enhancement observed for the hydrolysis of DPP$^-$ when compared to symmetric phosphodiesters with comparable leaving groups[7] and so is examined in more detail.

The transition state (TS) for the hydrolysis reaction by mechanism iv was verified by IRC calculations. The IRC profile (Figure 3) is consistent with a single step, concerted reaction, with two water molecules playing well-defined roles in TS1. (Cartesian coordinates for reactant, TS and product are given in the Supporting Information.)

To confirm the rate enhancement for DPP$^-$, we performed the same calculation (for the $S_N2(P)$ mechanism iiia) for the

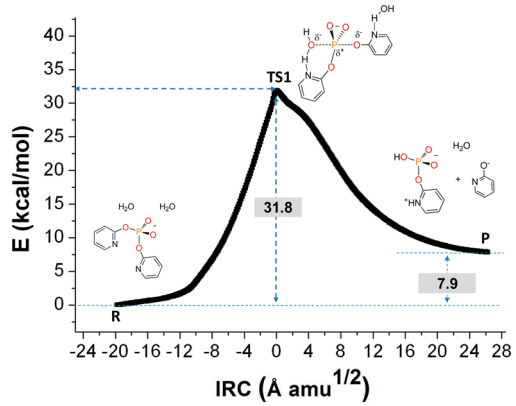

Figure 3. IRC profile for the hydrolysis reaction of DPP.

hydrolysis of bis-4-chlorophenyl phosphate 4ClPP in the presence of two to four discrete water molecules at 100 °C. The calculated free energy of activation is some 6 kcal·mol^{-1} higher than observed for the hydrolysis of DPP$^-$, giving a calculated rate close to that expected for 4ClPP$^-$ at 100 °C (Table 6).

Table 6. Activation Free Energies and Rate Constants for the Hydrolysis of 4ClPP by Mechanism iiia with Two, Three, and Four Discrete Water Molecules Present: Calculated at 100°C at the B3LYP/6-31++G(d,p) Level of Theory

no. of water molecules	10^{10} k_{calc} (s^{-1})	$\Delta G^{\ddagger}$ (kcal/mol)
mechanism iiia (2 H_2O)	1.84×10^{-7}	40.3
mechanism iiia (3 H_2O)	15.5	37.1
mechanism iiia (4 H_2O)	7.71	37.6
experimental (extrapolation)[7]	4.93	37.9

To allow a more detailed comparison of the reactions of DPP$^-$ and 4ClPP we also constructed the IRC (Figure 4) for

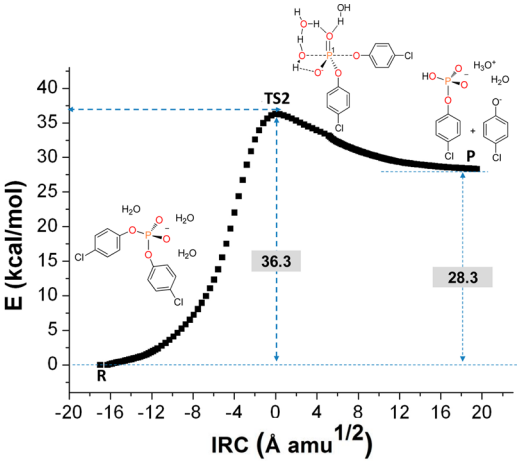

Figure 4. IRC profile for the hydrolysis reaction of 4ClPP.

the hydrolysis reaction of the latter, simple diaryl phosphate in the presence of three waters. The apparently high energy of the product with respect to reactant in Figure 4 is due to the fact that the proton transfer from hydronium (H_3O^+) to 4-chlorophenolate anion is not included in this step. The IRC confirms the concerted single-step pathway, with the three water molecules playing well-defined roles. In particular, the

dx.doi.org/10.1021/jo302498g | J. Org. Chem. 2013, 78, 1343–1353

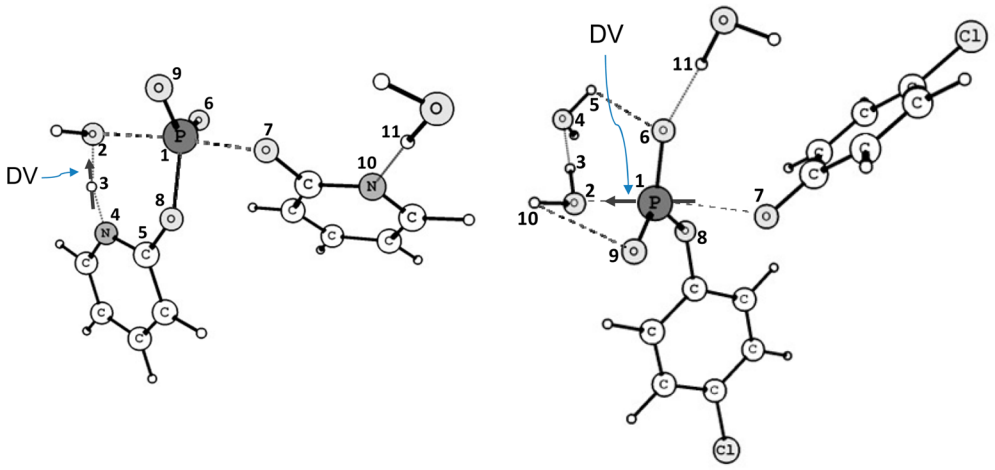

TS 1: DPP (ν_{ima}=666.24 i cm^{-1}) **TS 2: 4ClPP** (ν_{ima}=190.95 i cm^{-1})

Figure 5. Optimized structures for the transition states TS for the hydrolysis reactions of DPP and 4ClPP. For a key to the atom numbering, see Scheme 10. The roles of the water molecules are discussed in detail in the following section.

water molecule closest (and hydrogen-bonded) to the nucleophilic H_2O is acting as the immediate general base (Figure 5 and Scheme 10).

Scheme 10. Transition States for the Hydrolysis of DPP and 4ClPP Detailing the Atom-Numbering Scheme

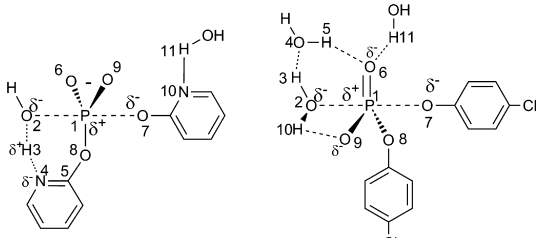

TS1: DPP TS2: 4ClPP

In each case, the hydrolysis reaction is initiated by the approach of an appropriately positioned solvent water molecule to the phosphorus center, to form a pentacoordinate transition state TS with a close to linear arrangement with the oxygen atom of the leaving group, as expected for a $S_N2(P)$ mechanism. The calculated angles $O_2\cdots P_1\cdots O_7$ are 171.6° and 172.57° for DPP and 4ClPP, respectively (Table 7), with imaginary frequencies of 666.24i and 190.95i corresponding to the rocking vibration leading to product formation. The displacement vector (DV) associated with the imaginary frequency is consistent in each case with a transition state in which P_1-O_2 formation and P_1-O_7 cleavage are concerted. The vectors are illustrated in Figure 5 to show the physical nature of the effect. The imaginary frequencies, the temperature of 100 °C, and the barriers including the zero-point energies (ZPE) for reactants, transition state, and product allow an estimate of the tunneling contribution for this reaction using the Truhlar derivation[21,22] and the Bell treatment.[23] The values obtained, 1.33 for DPP and 1.02 for 4ClPP, indicate that any tunneling contribution to this mechanism is negligible.

Bond Order Analysis. To compare bond order evolution in the transition state with respect to reactant, we performed a natural bond orbital (NBO) calculation as implemented in

Table 7. Structural Parameters for Reactant (R), Transition State (TS), and Product (P) at the B3LYP/6-31++G(d,p) Level of Theory[a]

	Interatomic Distances (Å)								
	DPP								
	P_1-O_2	O_2-H_3	H_3-N_4	N_4-C_5	C_5-O_8	P_1-O_7	P_1-O_8	P_1-O_6, P_1-O_9	$N_{10}-H_{11}$
R	3.55	0.98	1.95	1.33	1.38	1.66	1.67	1.51, 1.51	1.85
TS1	1.98	1.31	1.18	1.34	1.34	1.85	1.74	1.52, 1.52	1.80
P	1.64	1.91	1.03	1.35	1.33	2.98	1.73	1.50, 1.50	1.82
	4-ClPP								
	P_1-O_2	O_2-H_3	H_3-O_4	O_4-H_5	H_5-O_6	P_1-O_7	P_1-O_8	P_1-O_6, P_1-O_9	O_6-H_{11}
R	4.51	0.98	1.80	0.99	1.76	1.65	1.65	1.52, 1.50	1.82
TS1	1.93	1.02	1.56	0.97	3.08	2.41	1.63	1.50, 1.50	1.82
P	1.68	1.44	1.06	0.98	3.23	5.39	1.65	1.51, 1.50	1.80
					DPP			4-ClPP	
	angle $O_2-P_1-O_7$ of TS (deg)				171.6			172.6	
	imaginary frequency (cm^{-1})				666.24i			190.95i	

[a]The atom numbering is defined in Scheme 10.

dx.doi.org/10.1021/jo302498g | J. Org. Chem. 2013, 78, 1343−1353

Table 8. Wiberg Bond Indices for Reactant (R), Activated Complex (TS), and Product (P) at the B3LYP/6-31++G(d,p) Level of Theory

		P_1-O_2	O_2-H_3	H_3-N_4	N_4-C_5	C_5-O_8	P_1-O_7	P_1-O_8	S_y
DPP	B_i^R	0.0032	0.6726	0.0553	1.3974	0.9537	0.5988	0.5930	0.889
	B_i^{TS}	0.3613	0.2684	0.4498	1.2893	1.0603	0.4256	0.5140	
	B_j^P	0.6651	0.0379	0.6766	1.2392	1.1003	0.0169	0.5030	
	%E_v	**54.1**	**63.7**	**63.5**	**68.3**	**72.7**	**29.8**	**87.8**	
4ClPP	B_i^R	0.0004	0.6590	0.0646			0.6177		0.654
	B_i^{TS}	0.3433	0.5341	0.1367			0.1420		
	B_j^P	0.5906	0.1710	0.4825			0.0002		
	%E_v	**58.1**	**25.6**	**17.3**			**77.0**		

Gaussian 09.[24−27] Wiberg bond indices were estimated from population analysis. Bond-breaking and -making processes involved in the rate limiting step were examined by means of the synchronicity (Sy) concept proposed by Moyano et al.[28] The synchronicity parameter offers a measure of the concertedness of a reaction, varying from zero, in the case of an asynchronous process, to unity, for a perfectly synchronous process. The results are shown in Tables 8 and S2 (Supporting Information). Wiberg bond indices B_i were calculated for all the bonds involved in the hydrolysis reactions of DPP and 4ClPP, as indicated in Scheme 10. Bonds undergoing negligible changes were not considered.

Transition State and Mechanism. The similar interatomic distances P_1-O_2 of 1.98 Å and 1.93 Å in the transition states for the reactions of DPP and 4ClPP, respectively, indicate comparable amounts of bond formation to the incoming nucleophile: but the P_1-O_7 distances to the leaving group, at 1.85 and 2.41 Å (Table 7), differ substantially. Evidently the transition state for the phosphate transfer process is reached earlier for the more reactive DPP, consistent with the involvement of the pyridine nitrogen, which is a more effective because it is stronger general base compared with a second water molecule. Thus, proton transfer from the nucleophilic water to nitrogen is further advanced (O_2-H_3 increases from 0.98 to 1.31 Å in the transition state for the DPP reaction, compared with 1.02 Å for 4ClPP), as the developing positive charge is stabilized more effectively on nitrogen than by solvent water. The more effective general base catalysis is reflected also in the Wiberg bond indices (Table 8), which indicate that proton transfer to nitrogen in the TS for the DPP reaction is ca. 65% complete, while the proton transfers involved in the dispersal of the developing positive charge on the nucleophilic water clearly lag behind for the 4ClPP reaction.

The estimated bond orders for bond-making and -breaking in the transition state for the reaction of DPP involving IGBC indicate similar degrees of change ("evolution") for all but one of the bonds directly involved: giving a synchronicity parameter close to unity (S_y = 0.889). Most advanced are the changes more closely involved in general base catalysis, with proton transfer from O_2 to N_4 well advanced and the formation of the new P_1-O_2 bond over 50% complete. The bond P_1-O_8, nominally to the nonleaving group, actually shows the highest degree of evolution in the TS (87.8%, Table 8): because it is affected both directly by the decreasing electrophilicity of phosphorus and by the development of positive charge at N. Only the cleavage of the P_1-O_7 bond to the leaving group is not well developed (29.8%) at the point where the transition state is reached for this very slow reaction.

For 4ClPP, in contrast, P_1-O_7 cleavage is the most advanced coordinate (%E_v = 77.0), followed by P_1-O_2 bond formation (%E_v = 58.1) (Table 8). Here the (even slower) reaction is driven primarily by the (poor) leaving group. P−O bond making and breaking are more closely synchronous, but the proton transfers involving solvent water molecules necessary for general base catalysis lag behind. These differences are the likely basis for the low solvent deuterium isotope effect, k_{H2O}/k_{D2O} = 1.28 ± 0.22 at 25 °C, observed for the hydrolysis of DPP. It is recognized that the magnitudes of such effects can be reduced when there is a large difference in pK_a between the proton donor and acceptor, resulting in a very early or late transition state.[29] In the present case both requirements are satisfied: the (water) donor and pyridine acceptor pK_a s are 15.7 and 2.73, respectively; and the proton transfer of H_3 from O_2 to N_4 from is well over half complete in the transition state, as indicated by both bond length and bond order calculations (Tables 7 and 8, above).

CONCLUSIONS

The combined kinetic and calculational evidence leads to the firm conclusion that the spontaneous hydrolysis of DPP^- involves intramolecular general base catalysis by pyridine nitrogen. The substantial rate increase over expectation for a symmetrical diester with leaving groups of pK_a 9.09, ca. 3000-fold at 100 °C and at least 10000-fold at 25 °C, corresponds to an EM of at least 15 M at 25 °C, of the order expected for relatively efficient IGBC.[12]

The rate acceleration is fully accounted for by a favorable entropy of activation, consistent with the involvement of an intramolecular nitrogen as the general base. The surprisingly low solvent deuterium isotope effect, k_{H2O}/k_{D2O} = 1.28 ± 0.22 at 25°, finds close precedent in the hydrolysis of the ester 4-nitrophenyl 2-dimethylaminopropionate (Scheme 11), another system demonstrating IGBC because the structure rules out intramolecular nucleophilic catalysis; for which k_{H2O}/k_{D2O} = 1.4 at 39 °C.[30]

Scheme 11. IGBC by Tertiary Nitrogen Is Observed When the Nucleophilic Mechanism Is Ruled out by Strain in a Potential 4-Membered Ring Intermediate[30]

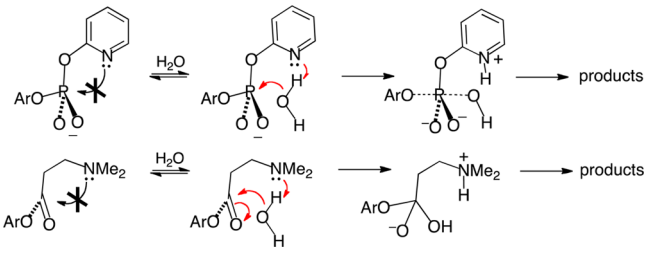

dx.doi.org/10.1021/jo302498g | J. Org. Chem. 2013, 78, 1343−1353

EXPERIMENTAL SECTION

General Methods. Organic solvents were carefully dried using molecular sieves (type 3A or 4A) and synthetic reactions carried out in strictly anhydrous conditions under argon. Chemicals and inorganic salts were of the highest purity available and were used as purchased. ^{1}H and ^{31}P NMR spectra were recorded on a spectrometer (400 and 200 MHz) with sodium 3-(trimethylsilyl) propionate (TSP) as internal reference for ^{1}H NMR and 85% phosphoric acid as external reference for ^{31}P NMR spectra. Chemical shifts are reported as δ (ppm). The time-of-flight (TOF) mass analyzer was used for HRMS measurements.

General Procedure for the Synthesis of Phosphate Diesters 2,4-DNPO-(PO_2^-)-OAr. A solution of 2,4-dinitrophenol (10 mmol) and triethylamine (10 mmol) in 20 mL of dry $CHCl_3$ was added dropwise to a cold solution of the appropriate phosphorochloridate (10 mmol, 4-nitrophenyl or phenyl−$OP(O)Cl_2$) in 30 mL of dry $CHCl_3$, and the reaction mixture was stirred overnight at room temperature. Unreacted chloride was hydrolyzed by adding triethylamine and water. This solution was extracted twice with $CHCl_3$ and the organic layer dried and evaporated. The diester was precipitated as the cyclohexylamine salt and recrystallized to give a colorless solid. **2,4-Dinitrophenyl phenyl phosphate** (2.28g, 52%): ^{1}H NMR (CD_3CN, 200 MHz) δ (ppm) 8.68 (d, 1H), 8.45 (dd, 1H), 7.85 (d, 1H), 7.31 (m, 2H), 7.14 (m, 3H); ^{31}P (CD_3CN, 200 MHz) δ (ppm) −13.6; ESI-MS negative-ion mode m/z calcd for $C_{12}H_8N_2O_8P^-$ 339.0, found 339.1 (100) $[M]^-$. **2,4-Dinitrophenyl 4-nitrophenyl phosphate** (2.13 g, 44%): ^{31}P (CD_3CN, 200 MHz) δ (ppm) −14.9 ppm; ESI-MS negative-ion mode m/z calcd for $C_{12}H_7N_3O_{10}P$ 383.9, found 384.0 (100) $[M]^-$.

Synthesis of Salts of Di-2-pyridyl Phosphate (DPP). A solution of 2-pyridone (2.48 g, 26.08 mmol) and triethylamine (2.63 g, 26.08 mmol) in 50 mL of dry THF was added dropwise under nitrogen to an ice-cooled solution of $POCl_3$ (2 g, 13.04 mmol) in 100 mL of dry THF. The reaction mixture was stirred for a further 15 min at 0 °C and then for 18 h at room temperature. Triethylamine (3 mL) in 20 mL of water was added and the reaction mixture stirred for 15 min. The THF was evaporated in vacuo and the remaining aqueous solution diluted with water then washed with CH_2Cl_2. After evaporationof the water, the crude product was dissolved in acetone and the triethylammonium chloride removed by filtration and evaporated to dryness. The product triethylammonium salt was dissolved in water and passed through an ion-exchange column (IR-120 resin, Na form) to give 2.43 g of DPP (Na salt, 68%): δH (250 MHz, D_2O) 8.10 (2H, dd, J = 5.33, 1.9 Hz), 7.74−7.81 (2H, m), 7.14−7.17 (2H, m), 7.10 (2H, d, J = 8.35 Hz); δP (250 MHz, D_2O) −11.90; ESI-MS positive-ion mode m/z calcd for $C_{10}H_8N_2O_4Na_2P$ 297.0017, found 297.0018 (100) $[M + Na]^+$.

Kinetic Methods. Reactions were initiated by adding 10 or 30 μL of a stock solution of the substrate DPP (5×10^{-3} M in water) to 1 or 3 mL of buffered aqueous solution at the appropriate pH. Buffers used were HCl (pH < 2), chloroacetate (pH 2−3.5), acetate (pH 4−5.5), Bis-TRIS (pH 6−7), TRIS (pH 8−9), CHES (pH 8.7 − 10.4), carbonate (pH ≈ 10), and KOH (pH >10). The reactions were followed, at constant temperature and ionic strength 1.0 (kept constant with KCl or NaCl, without significant difference in rate constants), by monitoring the appearance of pyridone at 294 nm on a spectrophotometer equipped with a thermostatted cell holder. Reactions at low pH (<3.5) and at pH > 12 were monitored to completion. At intermediate pH's, rate constants for the hydrolysis of DPP were determined by the initial rate method, using more concentrated solutions (5 to 15 mM) of substrate. In a typical run, 100 μL of 150 mM aqueous solution were added to 900 μL of a buffer solution equilibrated to the desired temperature. The absorbance of the released product was monitored by UV−vis spectroscopy at 294 nm. The observed rate constants were obtained by dividing the initial rates of change of absorbance by the final change in absorbance under the reaction conditions (hydrolysis of DPP produces 2 equiv of 2-pyridone in the acid-catalyzed and pH-independent regions, but 1 equiv at pH >10). The total change in the absorbance of hydrolysis of DPP was determined by hydrolyzing an aliquot of the reaction solution to completion in HCl and measuring the absorbance at the same pH in the same buffer solution as the original reaction.

At 25 °C, the DPP anion has a half-life of over 70 years, and more concentrated solutions cannot be used for initial rate measurements because the absorbance of the substrate (λ_{max} = 270 nm) overlaps with that of the released 2-pyridone. Thus, the appearance of 2-pyridone at 294 nm produces only very small changes over very long periods (typically 0.01 absorbance units over 2 days), placing this reaction on the borderline of what is measurable at 25 °C. Numerous measurements over 2 years, in our two different laboratories, in different hemispheres, produced constants in the k_0 (pH 9−10) region which we considered to be accurate to no more than an order of magnitude: these have been discarded. We are confident that the data cited in Table 1 are the best that can be obtained under these circumstances: and their validity is supported by the excellent agreement with data collected at higher temperatures (Table 2), as defined by an Eyring plot with r > 0.999.

The k_0 data at higher temperatures complement and support the results at 25 °C. pHs of buffer solutions were generally measured at 25 °C and the same conditions used at higher temperatures. Detailed measurements for the runs at 75 °C (Table 9) showed that the pH (and thus the apparent pK_a of the buffer) had shifted downward by some 1.2 units, but so too had the minimum in the pH profile for the reaction (Figure 6). Much of this shift can be attributed to the

Table 9. DPP Hydrolysis in CHES Buffer at 25 and 75 °C, I = 1.0 M[a]

[CHES] (mM)	pH	T (°C)	k_{obs} (s^{-1})
50	9.4	25	$2.0 \pm 0.2 \times 10^{-10}$
200	9.4	25	$1.4 \pm 0.2 \times 10^{-10}$
50	7.8	75	$3.2 \pm 0.03 \times 10^{-7}$
50	8.2	75	$1.6 \pm 0.02 \times 10^{-7}$
50	8.6	75	$1.1 \pm 0.01 \times 10^{-7}$
200	7.8	75	$2.6 \pm 0.02 \times 10^{-7}$
200	8.2	75	$1.5 \pm 0.01 \times 10^{-7}$
200	8.6	75	$1.1 \pm 0.01 \times 10^{-7}$

[a]Note: [DPP] = 15 mM. The total change in the absorbance at 294 nm is calculated for the formation of 2 equiv of 2-pyridone.

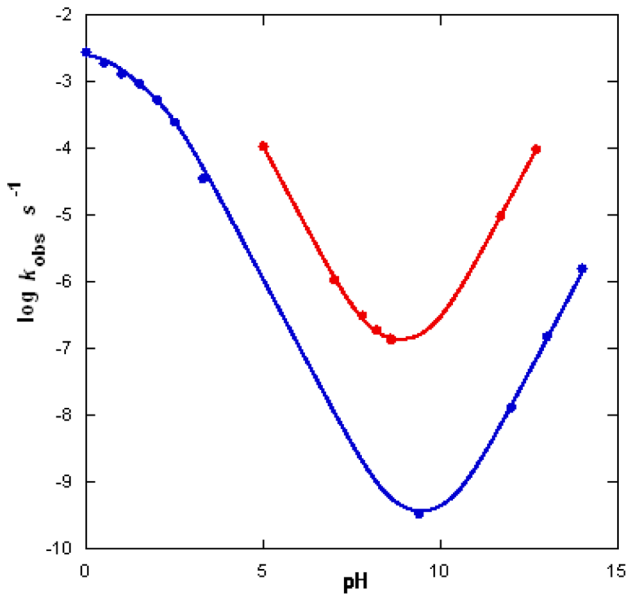

Figure 6. pH−rate profile for the hydrolysis of DPP at 75 °C compared with the same measured at 25 °C (from Figure 1).

dx.doi.org/10.1021/jo302498g | J. Org. Chem. 2013, 78, 1343−1353

decrease in pK_w (which falls from 14 at 25 °C to 12.24 at 100 °C).[31] The calculated curves are naturally shallow close to the pH minimum, where the rate is identical or very close to the pH-independent k_0; e.g. the rate difference at 75 °C between the observed minimum at about pH 8.87 and pH 9.4 (the minimum at 25 °C) is only some 20%. Thus, full pH–rate profiles were generally not measured at the highest temperatures.

The data shown in Table 9, at pH's 7.8, 8.2, and 8.6 (30, 50, and 70% free base buffer) measured at 75 °C demonstrate very clearly the absence of buffer catalysis. Rates are actually reduced at higher buffer concentrations, as they are also at higher pH, corresponding to the approach to the pH minimum.

The rate constant at 100 °C is based on an independent measurement in which the reaction was followed to completion by HPLC, in 70% free base CHES buffer (Figure 7).

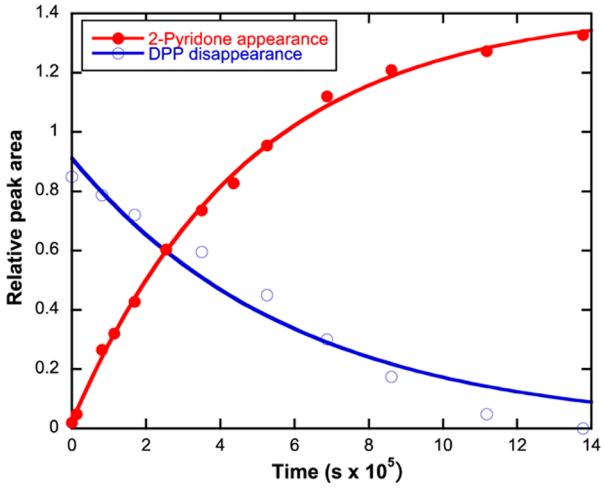

Figure 7. Spontaneous hydrolysis of DPP in CHES buffer (70% free base, I = 1.0 M KCl) at 100 °C, quantified by HPLC: ● = pyridone appearance at 224 nm, ○ = substrate disappearance at 275 nm.

Activation Parameters for DPP Hydrolysis. Activation parameters for the spontaneous hydrolysis of DPP were calculated from rate constants measured in CHES buffer (0.05 M, 70% free base, I = 1.0 M (KCl)) at 25, 45, 60, 75, and 90 °C (Table 2). At each temperature the initial rate of the reaction was monitored using UV–vis spectroscopy at 294 nm. At 100 °C, the reaction was followed to completion using HPLC. The observed first order rate constants for water attack and second order rate constants for hydroxide attack were analyzed by Eyring plots for the two reactions (see the Supporting Information).

■ ASSOCIATED CONTENT

Supporting Information

Tables and figures giving kinetic and theoretical study data. This material is available free of charge via the Internet at http://pubs.acs.org.

■ AUTHOR INFORMATION

Corresponding Author

*Tel: +55-48-3721-6849. Fax: +55-48-3721-6850. E-mail: faruk.nome@ufsc.br, ajk1@cam.ac.uk, N.H.Williams@sheffield.ac.uk.

Notes

The authors declare no competing financial interest.

■ ACKNOWLEDGMENTS

We are grateful to INCT-Catálise, PRONEX, FAPESC, CNPq, and CAPES in Brazil; to EPSRC (Engineering and Physical Sciences ResearchCouncil; EP/E01917X; UK); and to The Libyan Ministry of Higher Education (to A.A.) for support of this work.

■ REFERENCES

(1) Kirby, A. J.; Medeiros, M.; Oliveira, P. S. M.; Brandão, T. A. S.; Nome, F. *Chem.—Eur. J.* **2009**, *15*, 8475.
(2) Liu, J. Q.; Wulff, G. *J. Am. Chem. Soc.* **2008**, *130*, 8044.
(3) Albert, A.; Phillips, J. N. *J. Chem. Soc.* **1956**, 1294.
(4) Kirby, A. J.; Medeiros, M.; Oliveira, P. S. M.; Orth, E. S.; Brandão, T. A. S.; Wanderlind, E. H.; Amer, A.; Williams, N. H.; Nome, F. *Chem.—Eur. J.* **2011**, *17*, 14996.
(5) Brown, R. S.; Zamkanei, M. *Inorg. Chim. Acta* **1985**, *108*, 201.
(6) Kirby, A. J.; Younas, M. *J. Chem. Soc., Sect. B* **1970**, 1165.
(7) Kirby, A. J.; Younas, M. *J Chem Soc., Sect. B* **1970**, 510.
(8) Orth, E. S.; Brandao, T. A. S.; Souza, B. S.; Pliego, P. R.; Vaz, B. G.; Eberlin, M. N.; Kirby, A. J.; Nome, F. *J. Am. Chem. Soc.* **2010**, *132*, 8513.
(9) Wolfenden, R.; Ridgway, C.; Young, G. *J. Am. Chem. Soc.* **1998**, *120*, 833.
(10) Schroeder, G. K.; Lad, C.; Wyman, P.; Williams, N. H.; Wolfenden, R. *Proc. Nat. Acad. Sci. U.S.A.* **2006**, *103*, 4052.
(11) Orth, E. S.; Brandao, T. A. S.; Milagre, H. M. S.; Eberlin, M. N.; Nome, F. *J. Am. Chem. Soc.* **2008**, *130*, 2436.
(12) Kirby, A. J. *Adv. Phys. Org. Chem.* **1980**, *17*, 183.
(13) Lassila, J. K.; Zalatan, J. G.; Herschlag, D. *Annu. Rev. Biochem.* **2011**, *80*, 669–702.
(14) Frisch, M. J.; G. W. Trucks, H. B. S., Scuseria, G. E.; Robb, M. A.; Cheeseman, J. R.; Scalmani, G.; Barone, V.; Mennucci, B.; Petersson, G. A.; Nakatsuji, H.; Caricato, M.; Li, X.; Hratchian, H. P.; Izmaylov, A. F.; Bloino, J.; Zheng, G.; Sonnenberg, J. L.; Hada, M.; Ehara, M.; Toyota, K.; Fukuda, R.; Hasegawa, J.; Ishida, M.; Nakajima, T.; Honda, Y.; Kitao, O.; Nakai, H.; Vreven, T.; Montgomery, J. A., Jr.; Peralta, J. E.; Ogliaro, F.; Bearpark, M.; Heyd, J. J.; Brothers, E.; Kudin, K. N.; Staroverov, V. N.; Kobayashi, R.; Normand, J.; Raghavachari, K.; Rendell, A.; Burant, J. C.; Iyengar, S. S.; Tomasi, J.; Cossi, M.; Rega, N.; Millam, J. M.; Klene, M.; Knox, J. E.; Cross, J. B.; Bakken, V.; Adamo, C.; Jaramillo, J.; Gomperts, R.; Stratmann, R. E.; Yazyev, O.; Austin, A. J.; Cammi, R.; Pomelli, C.; Ochterski, J. W.; Martin, R. L.; Morokuma, K.; Zakrzewski, V. G.; Voth, G. A.; Salvador, P.; Dannenberg, J. J.; Dapprich, S.; Daniels, A. D.; Farkas, O.; Foresman, J. B.; Ortiz, J. V.; Cioslowski, J.; Fox, D. J. Gaussian 09, Revision A.02; Gaussian, Inc.: Wallingford, CT, 2009.
(15) McQuarrie, D. *Statistical Mechanics*, New York, 1986.
(16) Marenich, A. V.; Cramer, C. J.; Truhlar, D. G. *J. Phys. Chem. B* **2009**, *113*, 6378.
(17) Kirby, A. J.; Mora, J. R.; Nome, F. *Biochim. Biophys. Acta* **2013**, *1834*, 454–463.
(18) Mora, J. R.; Kirby, A. J.; Nome, F. *J. Org. Chem.* **2012**, *77*, 7061.
(19) (a) Iche-Tarrat, N.; Barthelat, J. C.; Rinaldi, D.; Vigroux, A. *J. Phys. Chem. B* **2005**, *109*, 22570. (b) Kamerlin, S. C. L.; Williams, N. H.; Warshel, A. *J. Org. Chem.* **2008**, *73*, 6960.
(20) Zhou, D. M.; Taira, K. *Chem. Rev.* **1998**, *98*, 991.
(21) Skodje, R. T.; Truhlar, D. G. *J. Phys. Chem.* **1981**, *85*, 624.
(22) Skodje, R. T.; Truhlar, D. G.; Garrett, B. C. *J. Phys. Chem.* **1981**, *85*, 3019.
(23) Caldin, E. F. *Chem. Rev.* **1969**, *69*, 135.
(24) Lendvay, G. *J. Phys. Chem.* **1989**, *93*, 4422.
(25) Reed, A. E.; Curtiss, L. A.; Weinhold, F. *Chem. Rev.* **1988**, *88*, 899.
(26) Reed, A. E.; Weinstock, R. B.; Weinhold, F. *J. Chem. Phys.* **1985**, *83*, 735.
(27) Wiberg, K. B. *Tetrahedron* **1968**, *24*, 1083.
(28) Moyano, A.; Pericas, M. A.; Valenti, E. *J. Org. Chem.* **1989**, *54*, 573.
(29) Grzyska, P. K.; Czyryca, P. G.; Purcell, J.; Hengge, A. C. *J. Am. Chem. Soc.* **2003**, *125*, 13106.

(30) Kirby, A. J.; Lloyd, G. J. *J. Chem. Soc., Perkin Trans. 2* **1976**, 1748.
(31) Whitfield, M. *J. Chem. Eng. Data* **1972**, *17*, 124.